LBL-33309
UC-414

Lawrence Berkeley Laboratory

UNIVERSITY OF CALIFORNIA

Accelerator & Fusion Research Division

Presented at the IEEE Particle Accelerator Conference, Washington, DC, May 17–20, 1993, and to be published in the Proceedings

Emittance Measurement and Modeling of the ALS 50 MeV Linac to Booster Line

J. Bengtsson, W. Leemans, and T. Byrne

May 1993

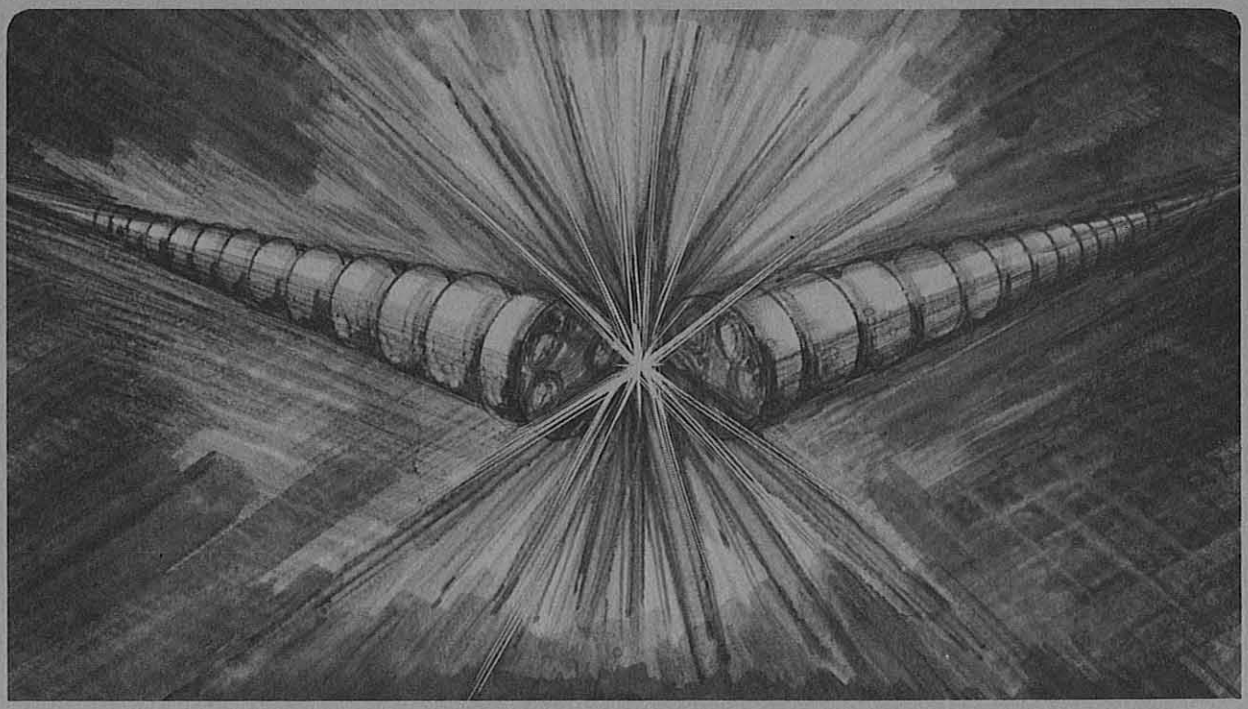

Prepared for the U.S. Department of Energy under Contract Number DE-AC03-76SF00098

DISCLAIMER

This document was prepared as an account of work sponsored by the United States Government. Neither the United States Government nor any agency thereof, nor The Regents of the University of California, nor any of their employees, makes any warranty, express or implied, or assumes any legal liability or responsibility for the accuracy, completeness, or usefulness of any information, apparatus, product, or process disclosed, or represents that its use would not infringe privately owned rights. Reference herein to any specific commercial product, process, or service by its trade name, trademark, manufacturer, or otherwise, does not necessarily constitute or imply its endorsement, recommendation, or favoring by the United States Government or any agency thereof, or The Regents of the University of California. The views and opinions of authors expressed herein do not necessarily state or reflect those of the United States Government or any agency thereof or The Regents of the University of California and shall not be used for advertising or product endorsement purposes.

Lawrence Berkeley Laboratory is an equal opportunity employer.

recycled paper

LBL-33309
UC-414

Emittance Measurement and Modeling of the ALS 50 MeV Linac to Booster Line

J. Bengtsson, W. Leemans, and T. Byrne

Accelerator and Fusion Research Division
Lawrence Berkeley Laboratory
University of California
Berkeley, California 94720

May 1993

This work was supported by the Director, Office of Energy Research, Office of High Nuclear Physics, High Energy Physics Division, of the U.S. Department of Energy under Contract No. DE-AC03-76SF00098.

LBL-33309
ESG-238

Emittance Measurement and Modeling of the ALS 50 MeV Linac to Booster Line *

J. Bengtsson, W. Leemans and T. Byrne
Lawrence Berkeley Laboratory, University of California
1 Cyclotron Road, Berkeley, CA 94720, USA

Abstract

The Twiss parameters and emittance have been measured for the ALS LINAC through non-linear χ^2 fitting of the measured beam size (fixed location) vs. focal strength of a quadrupole triplet. The obtained values have been used to calculate the expected beam size and dispersion along the linac-to-booster transport line giving good agreement with measurements. The efforts resulted in superior injection into the booster.

I. INTRODUCTION

The Advanced Light Source at LBL has a 50 MeV linac, a booster which increases the electron energy to 1.5 GeV and a storage ring which is expected to need refilling every 6 - 8 hours. In between refills the 50 MeV electron will be transported into an experimental vault and will be used to conduct a number of experiments such as plasma lens focusing, generation of femtosecond X-ray pulses and interaction of the electron beam with a variety of electromagnetic cavities [1].

To be able to design a beam transport line optimized for the different experiments, we have measured the beam's initial conditions after the linac. In addition, these values have also been used to calculate the beam size and dispersion along the Linac-To-Booster (LTB) transport line and compared with measurements.

II. THEORETICAL MODEL

A. Equations of motion

The linearized transverse motion of the beam is described by [2]

$$x(s) = \sqrt{\varepsilon_x \beta_x(s)} \cos[\mu_x(s) + \varphi_x] + \eta_x(s)\,\delta$$

using the phase space coordinates $\bar{x} = (x, p_x, y, p_y, \delta)$, where β is the beta-function, μ the phase advance, η the dispersion and ε a constant of motion known as the emittance. The beam is parameterized by the six parameters α_x, β_x, ε_x, α_y, β_y and ε_y at each point along the transport line. Since we have three parameters in each plane but can only observe configuration space, i.e. beam sizes, we need at least three different observations of beam size in each plane to be able to determine the corresponding beam parameters at a given point along the transport line.

B. Statistical Analysis by Non-linear χ^2

The horizontal beam size x is a function of α_x, β_x and ε_x

$$x(\bar{q}, \bar{a}) = \sqrt{\varepsilon_x \left[m_{11}^2 \beta_x(\bar{q}) - 2\, m_{11} m_{12} \alpha_x(\bar{q}) + m_{12}^2 \frac{1 + \alpha_x^2(\bar{q})}{\beta_x(\bar{q})} \right]}$$

with $\bar{a} = (\beta_x, \alpha_x, \varepsilon_x)$ as parameters, $\bar{q} = (q_f, q_d)$ as independent variables and m_{ij} being the elements of the transport matrix $\bar{x}_f = M\,\bar{x}_i$. The χ^2 merit function is

$$\chi^2(\bar{a}) = \sum_{i=1}^{N} \left[\frac{x_i - x(\bar{q}_i; \bar{a})}{\sigma_i} \right]^2$$

where N is the number of data points, i.e. measured and computed beam size. χ^2 is minimized by solving the system

$$\sum_{l=1}^{N} v_{kl}\, \delta a_l = u_k\,, \quad u_k \equiv -\frac{1}{2} \frac{\partial \chi^2}{\partial a_k} = \sum_{i=1}^{N} \frac{[x_i - x(\bar{q}_i; \bar{a})]}{\sigma_i^2} \frac{\partial x(\bar{q}_i; \bar{a})}{\partial a_k}$$

$$v_{kl} \equiv \frac{1}{2} \frac{\partial^2 \chi^2}{\partial a_k \partial a_l} = \sum_{i=1}^{N} \frac{1}{\sigma_i^2} \frac{\partial x(\bar{q}_i; \bar{a})}{\partial a_k} \frac{\partial x(\bar{q}_i; \bar{a})}{\partial a_l} + O(\partial^2)$$

and iterating [3]. The second order derivatives have been neglected to stabilize the iterations. We find

$$u_1 = -\frac{1}{2} \frac{\partial \chi^2}{\partial \beta_x} = \sum_{i=1}^{N} \frac{[x_i - x(\bar{q}_i; \bar{a})]}{\sigma_i^2} \frac{\varepsilon_x \left(m_{11}^2 - m_{12}^2 \frac{1 + \alpha_x^2(\bar{q}_i)}{\beta_x^2(\bar{q}_i)} \right)}{2\sqrt{}}\,,$$

$$u_2 = -\frac{1}{2} \frac{\partial \chi^2}{\partial \alpha_x} = \sum_{i=1}^{N} \frac{[x_i - x(\bar{q}_i; \bar{a})]}{\sigma_i^2} \frac{\varepsilon_x \left(-m_{11} m_{12} + m_{12}^2 \frac{\alpha_x(\bar{q}_i)}{\beta_x(\bar{q}_i)} \right)}{\sqrt{}}\,,$$

$$u_3 = -\frac{1}{2} \frac{\partial \chi^2}{\partial \varepsilon_x} = \sum_{i=1}^{N} \frac{[x_i - x(\bar{q}_i; \bar{a})]}{\sigma_i^2} \times \frac{m_{11}^2 \beta_x(\bar{q}_i) - 2\, m_{11} m_{12} \alpha_x(\bar{q}_i) + m_{12}^2 \frac{1 + \alpha_x^2(\bar{q}_i)}{\beta_x(\bar{q}_i)}}{2\sqrt{}}$$

where

$$\sqrt{} \equiv \sqrt{\varepsilon_x \left(m_{11}^2 \beta_x(\bar{q}_i) - 2\, m_{11} m_{12} \alpha_x(\bar{q}_i) + m_{12}^2 \frac{1 + \alpha_x^2(\bar{q}_i)}{\beta_x(\bar{q}_i)} \right)}$$

The confidence interval is given by

$$\delta a_i = \pm \sqrt{\Delta\chi^2 (v)^{-1}_{ii}}$$

where we choose $\Delta\chi^2 = 4$ for a 95.4 % confidence interval.

*This work was supported by the Director, Office of Energy Research, Office of Basic Energy Sciences, Materials Sciences Division, of the U.S. Department of Energy under Contract No. DE-AC03-76SF00098.

where we choose $\Delta\chi^2 = 4$ for a 95.4 % confidence interval.

III. EMITTANCE MEASUREMENT

A. Linac parameters

The parameters of the linac are given in Table 1. The LTB line transports the beam towards the 1.5 GeV booster and must be tuned to provide the correct matching conditions into the ring.

Maximum Energy	50 MeV
Charge	1-2 nC/bunch
Bunch Length (σ_z)	10-15 ps
Emittance rms (unnorm)	0.3 mm-mrad
# bunches/macro pulse @ 125 MHz	1 - 10 (max 100)
Macro pulse rep. rate	1 - 10 Hz

Table 1: ALS Linac parameters

Typically, emittance measurements are done with a pepper pot and beam profiles are measured with wire scans or harps. We have carried out the measurements by measuring the beam size on a fluorescent screen as a function of the focal strength of the focusing element, Q_{12}, of a quadrupole triplet, while keeping the defocusing element, Q_{11}, at a fixed strength.

The beam size is obtained as follows: light emitted by the fluorescent screen, is imaged onto a CCD-camera. The video signal output is frame-grabbed with 8 bit resolution on a Macintosh computer and analyzed using commercial image processing software. For the particular choice of magnification, the intrinsic spatial resolution of the system is about 110 μm but the statistical analysis, discussed previously, improves this about five-fold to 20 μm. For fixed imaging conditions, we have evaluated the linearity of the system by measuring the peak number of counts on the image as a function of number of bunches per macro pulse. The complete imaging system was found to be linear, for beam intensities below those resulting in 200 counts on the image. The noise floor is typically 15 counts.

After acquisition of an image, horizontal and vertical line-outs were fit to a Gaussian distribution using a non-linear Levenberg Marquardt fitting routine [3] with 3 parameters: noise floor (counts), amplitude (counts) and rms beam size.

C. Emittance measurement.

The measurements were carried out as follows. First, all quadrupole magnets were cycled. At the end of the cycling procedure the current was brought up to 90 % of the final set-value and then slowly increased to the 100% value. Without these procedures, preliminary measurements indicated that hysteresis effects led to irreproducible results. For a given current setting of the focusing (defocusing) element, the current delivered to the defocusing (focusing) element was varied from 0 to 8 A (maximum current) in steps of 0.5 A. An example of the horizontal and vertical beam sizes as a function of current is shown in Fig. 1.

The experimental results were modeled with TRACY [4] using the measured location of the different beam line components (dipole and quadrupole magnets, fluorescent screens); magnetic lengths and strengths. The magnetic length for each quadrupole was calculated from the measured $B'L_{eff}$ line integral value and the calculated field gradient, for a given current setting. All the current supplies were carefully calibrated. The measured transfer functions of the quadrupoles were used to calculate the focusing strength .

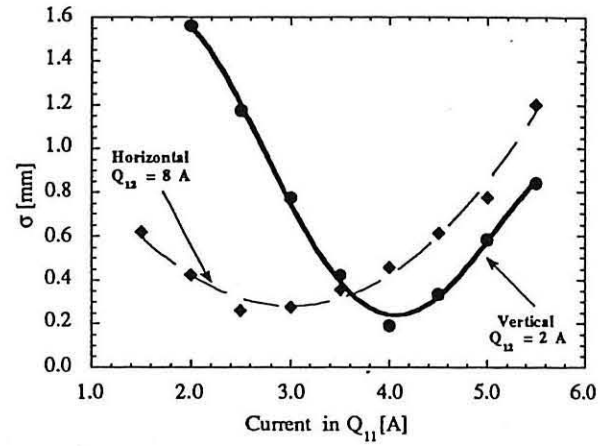

Figure 1: Horizontal and vertical beam sizes as a function of current in Q_{11} for fixed current in Q_{12}. The lines through the data are polynomial fits used in the modeling.

The results of the non-linear χ^2 from are summarized in Table 2.

α_x	1.31 ± 0.12
β_x [m]	3.09 ± 0.29
ε_x rms, unnorm. [mm-mrad]	0.32 ± 0.02
α_y	-0.19 ± 0.11
β_y [m]	1.00 ± 0.10
ε_y rms, unnorm. [mm-mrad]	0.33 ± 0.03

Table 2: Measured initial conditions for the 50 MeV beam.

IV. MODELING OF THE LTB-LINE

The measured initial conditions allow us to calculate the beam sizes and dispersion along the linac-to-booster (LTB) line and to compare with measured values. Previous operation of the LTB-line utilized quadrupoles set points giving predicted beam sizes shown in Fig. 2. Visual inspection of beam profiles, aided by image enhancing software, indicated beam scraping. Furthermore, one could also notice considerable beam motion at the injection point. This is explained by rather large dispersion at that point and the pulse to pulse energy jitter of the linac.

However, the measured initial conditions allow us to calculate the proper settings of the quadrupole power supplies for matching the beam into the booster. The beam profiles were measured at 5 different locations along the LTB-line for these settings. The comparison between experimental and theoretical results is given in Table 3. Notice, that a small modeling error of the dispersion at one point will be substantially magnified in downstream quadrupoles. No

fluorescent screen is present after B1 preventing us from measuring dispersion after the achromat (BS, Q2 and B1).

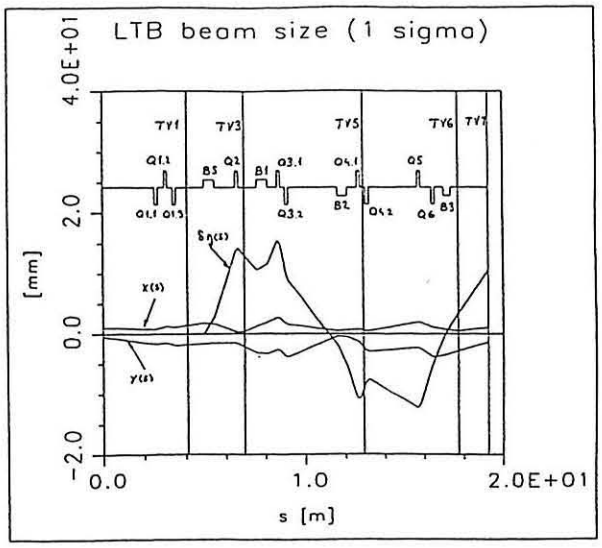

Figure 2: Original predicted beam profile along the LTB line and the effect of dispersion.

The predicted beam profiles for the optimized settings are shown in Fig. 3.

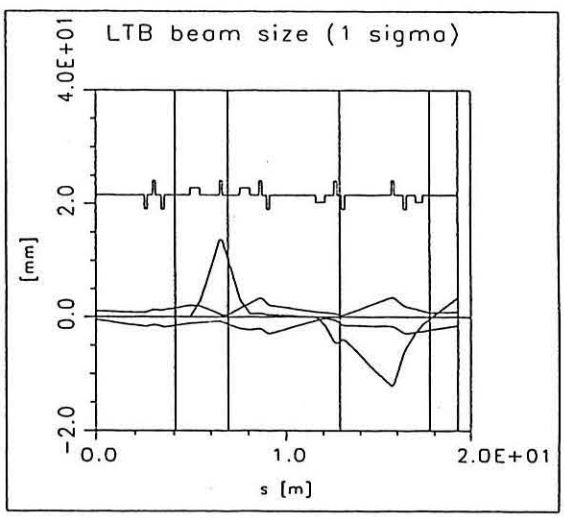

Figure 3: Optimized LTB-line, tuned for minimum dispersion at injection into the booster.

The experimentally measured vertical beam sizes is given by $\sigma = \sqrt{\varepsilon\,\beta}$. However, analysis of the horizontal beam profiles is complicated by the fact that beam loading of the accelerator structure leads to systematic energy difference between consecutive bunches of 0.8 %. This causes only partial spatial overlapping of the beam profiles on screens located in dispersive sections. The need for running more than 1 bunch arose from the limited light sensitivity of the imaging system. With the present LINAC performance, adding consecutive images to increase the dynamic range cannot be done: the energy jitter between consecutive macro-pulses was found to be as high as 1%. We are currently working on improving the sensitivity of the imaging system by an order of magnitude.

Loc.	Measured σ_{hor} [mm]	Model σ_{hor} [mm]	Measured σ_{ver} [mm]	Model σ_{ver} [mm]
tv1	1.67	1.53, 1.53	1.76	1.52
tv3	9.15	10.69, 0.33	1.16	1.28
tv4	2.88	4.69, 0.37	0.99	1.06
tv5	2.49	1.08, 0.70	1.76	2.36
tv6	0.81	4.30, 0.88	1.30	1.52

Table 3: Experimental and theoretical beam sizes along the LTB-line. The first and second entry in the third column are with and without dispersion taking into account, respectively.

To obtain the linear dispersion, the change of beam location Δx on TV3 (Q2 off) was measured as a function of the strength of the upstream BS dipole magnet. By using

$$\Delta x = \delta\,\eta_x = \delta\left[\rho_0(1 - \cos\phi) + L_{drift}\sin\phi\right],$$

$$\delta = -\,\Delta B_\perp \frac{\rho_0}{(B_\perp\,\rho)_0} + O(2)$$

we find a measured dispersion $\eta_x = 1.18$ m which agrees well with the predicted value of 1.13 m.

CONCLUSIONS

A detailed quantitative analysis has been presented on a) the measurement of the beam emittance and Twiss parameters of the ALS Linac, and b) on the modeling and optimization of the LTB line. The solution for the beam's initial conditions was propagated down the LTB-line. Good agreement between the calculated and measured beam sizes and dispersion was obtained. Furthermore, the quantitative and qualitative analysis of beam profiles helped us to diagnose incorrect operation of the Linac sub-harmonic bunching system, calibration problems with power supplies and.the importance of magnet cycling to avoid systematic errors caused by hysteresis effects. Finally, it has led to a substantial improvement of injection stability of the beam into the booster.

ACKNOWLEDGMENT

The authors would like to thank S. Chattopadhyay and the Center for Beam Physics for continuos support and encouragement, and the ALS operations team for their cooperation.

REFERENCES

[1] W. Leemans et al., these proceedings.
[2] E. D. Courant and H. S. Snyder, Ann. Phys. Vol 3, p. 1 (1958).
[3] W. H. Press, B. P. Flannery, S. A. Teukolsky and W. T. Vetterling, "Numerical Recipes" (Cambridge University Press) 1989.
[4] J. Bengtsson, E. Forest and H. Nishimura, unpublished.